Pergamon

Bioorganic & Medicinal Chemistry Letters 9 (1999) 1963–1968

BIOORGANIC & MEDICINAL CHEMISTRY LETTERS

CORRELATION OF ANTI-HIV ACTIVITY WITH STRUCTURE: USE OF ELECTROSTATIC POTENTIAL AND CONFORMATIONAL ANALYSIS

Travis Mickle and Vasu Nair*

Department of Chemistry, The University of Iowa, Iowa City, IA 52242, U.S.A.

Received 20 April 1999; accepted 26 May 1999

Abstract: Electrostatic potential distribution, 3-D electron density shapes, and conformational analysis were used to correlate anti-HIV activity or inactivity of AZT, (-) carbovir, oxetanocin A, and 16 isomeric dideoxynucleosides of different families. The structure–activity profile discovered is significant and is expected to contribute to the development of a much needed predictive QSAR analysis in this area.

Introduction

The ability to correlate anti-HIV activity with structure and stereochemistry of nucleosides and nucleotides is of considerable significance, not only to contribute to the detailed understanding of the mechanism of action of these compounds, but also to provide predictive information on structural characteristics most likely to elicit activity. Yet, in the case of anti-HIV active dideoxynucleosides, QSAR correlations have not been proposed. An approach with some limited success involves correlation of activity with conformation,[1-3] the latter being defined in terms of the glycosidic torsional angle, orientation of the 5′-OH, and sugar ring puckering.[4] Examination of electrostatic potential combined with other properties (e.g., conformation, electronic effects of electrostatic potential, hydrophobicity, lipophilicity, and hydrogen-bonding sites) has suggested that if molecules have similar electrostatic potential, along with these key properties, then it is more probable that their molecular recognition by enzymes and receptors would be alike.[5,6] Also, in the case of anti-HIV active nucleosides, phosphorylation to the triphosphate is a requirement for inhibition of HIV reverse transcriptase (HIV RT), and even rudimentary studies of docking at the active site of HIV RT would require extensive modeling work with many assumptions. Docking studies with the phosphorylating kinases would be even more difficult as the crystal structures of some of these enzymes have not been determined. However, using electrostatic potential, fundamental structural properties can be examined for a qualitative correlation. Areas of high, neutral, and low electrostatic potential can be determined for active nucleosides and nucleotides. The binding site within relevant enzymes would then be expected to have opposite areas of electrostatic potential.

We have investigated recently the synthesis and anti-HIV activity of isomeric dideoxynucleosides (isoddNs, Figure 1), that is, dideoxynucleosides with transposed base moieties or transposed -CH_2OH groups.[7] One of these isomeric nucleosides, (*S,S*)-isoddA, **2**, has potent anti-HIV activity against HIV-1 and HIV-2.[8] Its

0960-894X/99/$ - see front matter
PII: S0960-894X(99)00324-8

triphosphate is one of the most powerful inhibitors of HIV RT known (K_i = 16 nM).[8] The enantiomer, (*R,R*)-isoddA, **3**, also shows some activity against HIV.[9] In comparison, none of the other isomeric nucleosides of the (*S,S*) and (*R,R*) or the apio families had significant anti-HIV activity.[7] The antiviral data for these compounds provide a unique opportunity to investigate the usefulness of electrostatic potential and conformational analysis to correlate anti-HIV activity of normal and isomeric dideoxynucleosides. This is the focus of the paper.

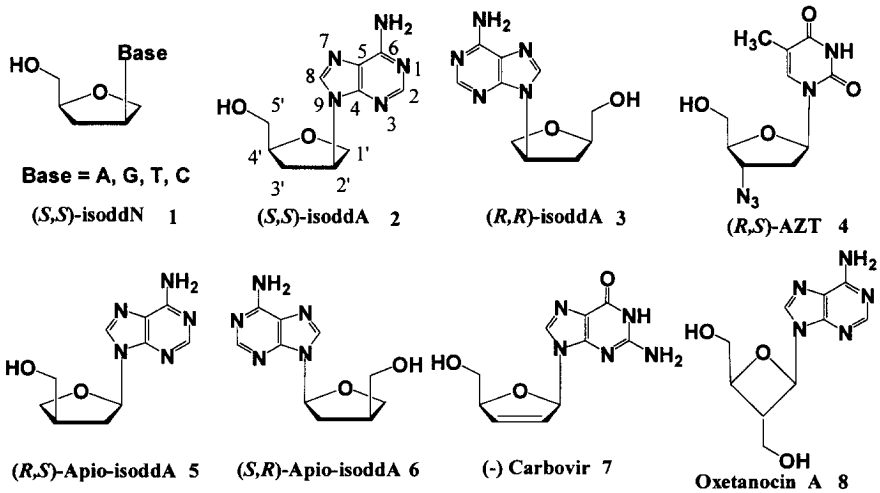

Figure 1. Structures and absolute stereochemical representations of examples investigated.

Materials and Methods

Molecular modeling of the nucleoside derivatives was carried out on a Silicon Graphics IRIS 4000/5000 system using the SYBYL program (Version 6.4; Tripos Associates, St. Louis, MO). The structures were first fully minimized to their lowest energy using the Powell method and charges were considered using the Gasteiger–Huckel charge calculation. The Gasteiger–Huckel charge calculation can give more accurate results in nucleosides where hydrogen bonding between 5'OH and O2 can take place. To construct the electrostatic potential surfaces, the partial charges were calculated using the Gasteiger–Marshalli method. Then, the electron density was calculated using a resolution of seven followed by the mapping of electrostatic potential on the surface of this electron density. Surfaces were then compared using their fully minimized structures. For the conformational analysis, a total of 1369 conformations (37^2, 0° and 360° were confirmed by re-calculation) were generated and their energies were fully minimized using GRID search. Both γ and χ were defined and searched through a full 360° range, with 10 degree increments. Each conformation gave an energy value and these values were graphed in terms of γ and χ using the TABLE and GRAPH option in SYBYL.

Results and Discussion

Electrostatic Potential. Examination of the electrostatic potential of (*S,S*)-isoddA (**2**) versus various other dideoxynucleosides shows some remarkable correlations. For example, comparison of (*S,S*)-isoddA (**2**) and (*R,S*)- or β-D-AZT (**4**) show that both molecules, in addition to having similar overall 3-D electron density

shapes in their most stable conformations, also exhibit similar regions of high (red, positive) and low (purple, negative) electrostatic potential (Figure 2). For purposes of comparison and correlation, we have examined only the key regions on the surface map and have allowed for small deviations resulting from rotational freedom about the glycosidic bond. Examination of AZTTP and (*S,S*)-isoddATP, the actual cellular inhibitors of HIV RT, show that they also have similar 3-D electron density surfaces and similar high and low regions of electrostatic potential distribution (Figure 3).

With the knowledge that two anti-HIV active molecules may show similar electrostatic potential surfaces, an analysis of some active and inactive compounds was conducted. As expected, (*S,S*)-isoddA (**2**) and its mirror image (*R,R*-isomer, **3**), demonstrated different 3-D electron density shapes and different electrostatic potentials (Figure 4). Neither the electrostatic potential distribution nor the conformational map (discussed below) in the case of (*R,R)*-isoddA correlated with AZT. To further confirm these findings, D- and L-related apio-series of isoddA [(*R,S*) and (*S,R*), **5** and **6**, respectively], which were both found to be inactive,[7] were compared to (*S,S*)-isoddA. Again, the 3-D electron density shapes were clearly different and the electrostatic potential surfaces also had some significant differences (Figure 5). Remarkable differences were also apparent within the (*S,S*)-isoddN group (**1**), which is consistent with the anti-HIV data which showed that none of the compounds with bases other than adenine had activity.[7] For example, comparison of (*S,S*)-isoddA (**2**) and (*S,S*)-isoddG (**1**, base = G) showed that both molecules had similar 3-D electron density shapes but completely different electrostatic potentials (Figure 6). Comparison of (*S,S*)-isoddA (**2**) with (*S,S*)-isoddC and (*S,S*)-isoddT (**1**, base = C and T) showed that, with the exception of the base region, they all have similar 3-D shapes and similar electrostatic potentials but the anti-HIV data show that only (*S,S*)-isoddA is active. Conformational data (see below) aided further in explaining the inactivity of (*S,S*)-isoddC and (*S,S*)-isoddT. Interestingly, the anti-HIV active carbocyclic nucleoside, (-) carbovir (**7**), and its triphosphate exhibited similar electrostatic potential distributions as (*S,S*)-isoddA and (*S,S*)-isoddATP, respectively (Figure 7). The anti-HIV active oxetanocin A, **8**, also had similar electrostatic potential to (*S,S*)-isoddA, AZT, and (-) carbovir (Figure 8). The similarity of the electrostatic potential surfaces of the triphosphates of oxetanocin A and (*S,S*)-isoddA is illustrated in Figure 9.

Conformational Analysis. To examine conformation, two torsional angles, χ and γ, were varied and the structure was minimized to give the lowest energy conformation of the sugar ring. For the isomeric nucleosides, the torsional angle χ was defined as the angle created by C2-N1-C2′-C1′. A map was generated using the two torsional angles as the x and y axis while energy was plotted along the z axis. Examination of the conformational maps of the anti-HIV inactive (*S,S*)-isoddC and the anti-HIV active ddC demonstrated that they are clearly different (Figure 10). Among the major differences are the relatively larger number of less favorable conformations (red and yellow regions) in (*S,S*)-isoddC versus ddC and their corresponding locations. Also, (*S,S*)-isoddC shows an interesting feature in its conformational map in that there is a local minimum (γ = -50, χ = -180 → -120, -50 → 0, 50 → 100, 150 →180) located within a less favorable conformational region.

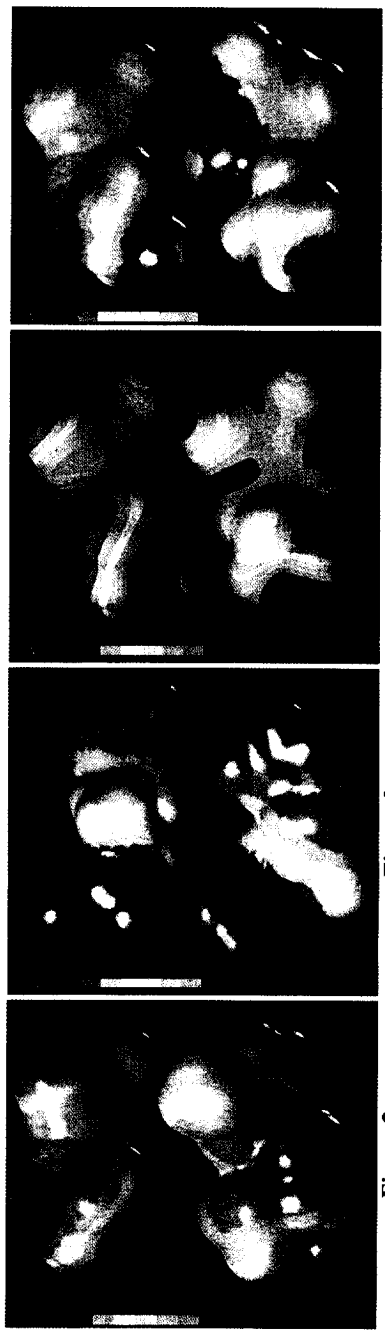

Figure 2

Figure 3

Figure 4

Figure 5

Figure 6

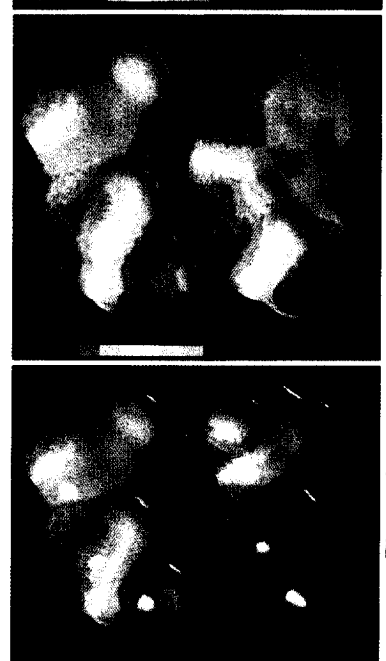

Figure 7

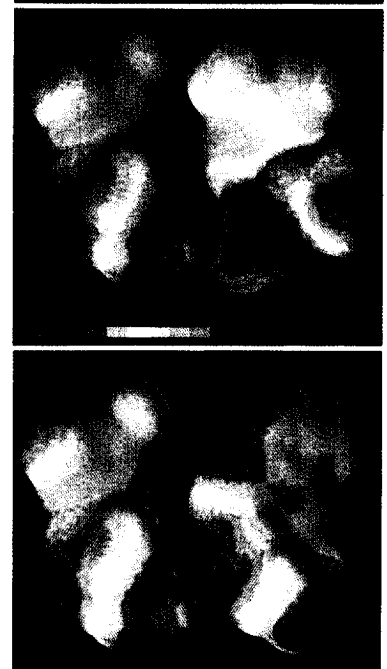

Figure 8

Figure 9

Figure 2. Electrostatic Potential Surfaces of (*S,S*)-isoddA (top) and AZT (bottom). **Figure 3.** Electrostatic Potential Surfaces of (*S,S*)-isoddATP (top) and AZTTP (bottom). **Figure 4.** Electrostatic Potential Surfaces of (*S,S*)-isoddA and (*R,R*)-isoddA (bottom). **Figure 5.** Electrostatic Potential Surfaces of (*S,S*)-isoddA (top) and (*R,S*)-apio-isoddA (bottom). **Figure 6.** Electrostatic Potential Surfaces of (*S,S*)-isoddA (top) and (*S,S*)-isoddG (bottom). **Figure 7.** Electrostatic Potential Surfaces of (*S,S*)-isoddA (top) and (-) carbovir. **Figure 8.** Electrostatic Potential Surfaces of (*S,S*)-isoddA (top) and oxetanocin A (bottom). **Figure 9.** Electrostatic Potential Surfaces of (*S,S*)-isoddATP and oxetanocin ATP (bottom). Note: Electrostatic potentials are measured on a relative scale located on the left-hand side of each figure. High (positive) regions of electrostatic potential are designated in red while low (negative) regions are indicated in purple.

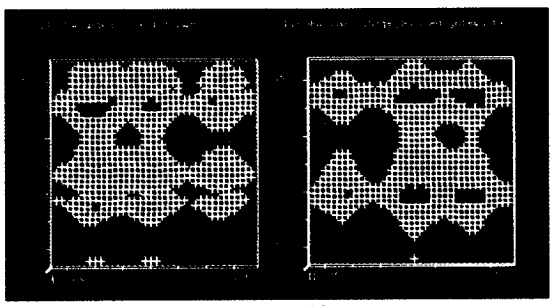

Figure 10

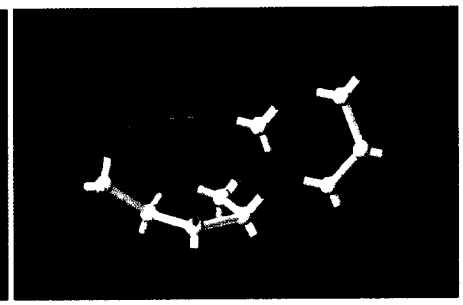

Figure 11

Figure 10. Conformation map of (*S,S*)-isoddC (left) and ddC (right). **Figure 11.** Minimized structure of (*S,S*)-isoddC showing hydrogen bonding between the 5'-OH and O-2 of cytosine moiety.

Within this local minimum region, there are several conformations that show relatively small 5'OH – O2 distances, which would suggest the presence of hydrogen bonding (Figure 11). Interestingly, examination of ddC conformations also shows that it can participate in this type of hydrogen bonding. However, the difference between isoddC and ddC is the stabilization that occurs through hydrogen bond formation (Table 1). Analysis of (*S,S*)-isoddT showed similar results (ΔE 2.350 kcal/mol). Differences in stability arising from hydrogen bond formation have been well documented.[10] Finally, the anti-HIV inactive (*R,S*)- and (*S,R*)-apio-isoddAs (**5** and **6**) demonstrated little correlation with (*S,S*)-isoddA (**2**) with respect to conformational energy maps, in contrast to the similarity of these maps for (*S,S*)-isoddA and other anti-HIV active ddNs such as ddC.

Table 1. Hydrogen bonding stabilization data.

Compound	Energy Before (in kcal/mol)	Energy After (in kcal/mol)	Δ E (in kcal/mol)	Angle of 5'-OH and O-2 (°)	H–Bond Distance (°A)
(*S,S*)-isoddA	11.000	7.429	3.571	148.56	1.787
ddC	15.282	13.809	1.473	150.86	1.773

In summary, examination of the anti-HIV activity of some isomeric and normal ddNs[11–16] and their electrostatic potential and conformational data reveals some interesting correlations (Table 2). The electrostatic potential surface of (*S,S*)-isoddA and its triphosphate show remarkably similar regions of high and low electrostatic potential as AZT and its triphosphate and oxetanocin A and its triphosphate. This may indicate that AZTTP, (*S,S*)-isoddATP, and oxetanocin A TP proceed through related binding mechanisms for anti-HIV activity. The inactivity of (*S,S*)-isoddC and (*S,S*)-isoddT can be correlated convincingly through their conformational energy maps. Examination of another isomeric series, the anti-HIV inactive apio-ddNs, indicates that there is a clear difference in electrostatic potential, 3-D electron density shape and conformation compared to the anti-HIV active isoddNs. Finally, the structure-activity profile discovered has significant ramifications and is expected to contribute to the development of a much-needed, predictive QSAR analysis in this area.

Acknowledgment: We thank the NIH for support of our research investigation (AI 32851).

Table 2. Structure–activity relationship involving electrostatic potential, conformation and anti-HIV activity

Molecules Examined	Electrostatic Potential Surfaces Similar To:	Conformation Map Similar To:	Active or Inactive	Anti-HIV-1 Data IC_{50} (μM)	Cell Line and Reference
β-D-AZT **4**	(S,S)-isoddA, (-) Carbovir, Oxetanocin A	None	Active	0.004 0.4	PBM (11) ATH8 (12)
(-) Carbovir **7**	AZT, (*S,S*)-isoddA, Oxetanocin A	D4T	Active	0.19 0.19	ATH8 (13) MT-2 (14)
(*S,S*)-isoddA **2**	AZT, (-) Carbovir, Oxetanocin A	ddC	Active	0.67	PBM (8)
(*S,S*)-isoddC **1**, base = C	(*S,S*)-isoddA (Some Similarity)	None	Inactive	>200	MT-4 (7)
(*S,S*)-isoddT **1**, base = T	(*S,S*)-isoddA (Some Similarity)	None	Inactive	>200	MT-4 (7)
(*S,S*)-isoddG **1**, base = G	None	None	Inactive	>200	MT-4 (7)
(*R,R*)-IsoddA **3**	None	None	Moderately Active	5-15 43	ATH8 (9) MT-4 (15)
(*S,R*)-apio-ddA, **6**	None	None	Inactive	>200	MT-4 (7)
(*R,S*)-apio-ddA, **5**	None	None	Inactive	>200	MT-4 (7)
Oxetanocin A **8**	AZT, (*S,S*)-isoddA, (-) Carbovir	None	Active	4	MT-4 (16)

References

1. Marquez, V. E.; Ezzitouni, A.; Russ, P.; Siddiqui, M. M.; Ford, H,; Feldman, R. J.; Mitsuya, H.; George, C.; Barchi, Jr., J. J. *J. Am. Chem. Soc.* **1998**, *120*, 2780.
2. Van Roey, P.; Salerno, J. M.; Chu, C. K.; Schinazi, R. F. *Proc. Natl. Acad. Sci. U.S.A.*. **1989**, *86*, 3929.
3. Bolon, P. J.; Nair, V. *Mag. Res. Chem.* **1996**, *34*, 243.
4. Altona, C.; Sundaralingam, M. *J. Am. Chem. Soc.* **1972**, *94*, 8205.
5. Richards, W. G., Ed.; *Computer-aided Molecular Design*. IBC Technical Services Ltd.: London, 1989.
6. Bagdassarian, C. R.; Schramm, V. L.; Schwartz, S. D. *J. Am. Chem. Soc.* **1996**, *118*, 8825.
7. Nair, V.; Jahnke, T. S. *Antimicrob. Agents Chemother.* **1995**, *39*, 1017, and references therein.
8. Nair, V.; St. Clair, M. H.; Reardon, J. E.; Krasny, H. C.; Hazen, R. J.; Paff, M. T.; Boone, L. R.; Tisdale, M.; Najera, I.; Dornsife, R. E.; Averett, D. R.; Borroto-Esoda, K.; Yale, J. L.; Zimmerman, T. P.; Rideout, J. L. *Antimicrob. Agents Chemother.* **1995**, *39*, 1993.
9. Huryn, D. M.; Sluboski, B. C.; Tam, S. Y.; Weigele, M.; Sim, I.; Anderson, B. D.; Mitsuya, H.; Broder, S. *J. Med. Chem.* **1992**, *35*, 2347.
10. Saenger, W. *Principles of Nucleic Acid Structure*, Springer-Verlag: NewYork, NY., 1984.
11. Chu, C. K.; Schinazi, R. F.; Arnold, B. H.; Cannon, D. L.; Doboszewski, B.; Bhadti, V. B.; Gu, Z. *Biochem. Pharmacol.* **1988**, *37*, 3543.
12. Mitsuya, H.; Weinhold, K. J.; Furman, P. A.; St. Clair, M. H.; Lehrman, S. N.; Gallo, R. C.; Bolognesi, D.; Barry, D. W.; S. Broder. *Proc. Natl. Acad. Sci. U.S.A.* **1985**, *82*, 7096.
13. Vince, R.; Brownell. J. *Biochem. Biophys. Res. Commun.* **1990**, *168*, 912.
14. Coates, J. A. V.; Cammack, N.; Jenkinson, H. J.; Mutton, I. M.; Pearson, B. A.; Storer, R.; Cameron, J. M.; Penn. C. R. *Antimicrob. Agents Chemother.* **1992**, *36*, 202.
15. Jones, M. F.; Nobel, S. A.; Robertson, C. A.; Storer, R.; Highcock, R. M.; Lamont, R. B. *J. Chem. Soc. Perkin Trans. I* **1992**, 1427.
16. Seki, J-L.; Shimada, N.; Takahashi, K.; Takita, T.; Takeuchi, T.; Hoshino, H. *Antimicrob. Agents Chemother.* **1989**, *33*, 773.